σ-bond expression for an analytic bond-order potential: Including π and on-site terms in the fourth moment

Volker Kuhlmann and Kurt Scheerschmidt*

Max Planck Institute of Microstructure Physics, Weinberg 2, 06120 Halle, Germany
(Received 21 November 2006; revised manuscript received 8 March 2007; published 31 July 2007)

An improved expression for σ bonds in *sp*-valent systems is derived for the analytical bond-order potential to four levels. The enhancement concerns the evaluation of the fourth moment of the local density of states with on-site and π terms. The latter introduce a torsional stiffness to the σ-bond order, previously known only for the π-bond order. The relative strength of the π enhancement as compared to the pure σ terms depends on the ratio of the π- and σ-bond integrals of the specific system. In the cubic diamond phase it is large for silicon (48%) and rather small for carbon (5%). The potential parameters are given for silicon and the predicted properties are compared with *ab initio* calculations and experimental data.

I. INTRODUCTION

To study atomic processes at nanoscopic time and length scales via molecular dynamics (MD) simulation,[1] accurate empirical potentials are needed. For example, such studies could deal with the relaxation of quantum dots or surface interactions during wafer bonding, and usually consider more than 10^5 atoms, which makes an exact description on the electronic level impossible. Such an interatomic potential would have predictive rather than descriptive character, if it was nevertheless derived from the underlying Schrödinger equation describing the electronic system. In doing so, it can be recognized as the ultimate goal to retain only the essential electronic information relevant to atomic bonding. As a link between the electronic and atomistic realms the tight-binding (TB) approximation[2] has proven to be successful. However, due to the cubic scaling behavior its application is limited to a few thousands of atoms. In the past various methods have been devised that aim to provide linear scaling by solving the TB Hamiltonian approximately.[3]

In the bond-order potential (BOP) the moments theorem is employed to derive[4,5] an analytical expression for the electronic bond order in terms of a many-atom expansion. After introducing the reduced TB model in Sec. II we present the approximations of the BOP in Sec. III. In Sec. IV we derive the extensions to the expansion of the σ-bond order. The resulting potential is parametrized for silicon in Sec. V.

II. REDUCED TIGHT-BINDING APPROXIMATION

Within the two-center, orthogonal TB model the cohesive energy can be split into three contributions:[6]

$$U_{\text{coh}} = U_{\text{rep}} + U_{\text{prom}} + U_{\text{bond}}. \tag{1}$$

The repulsive energy can be represented by a local embedding function[7] with a pairwise potential ϕ_{ij}, whose distance dependence is described by a scaling function $s(r_{ij})$ and separated from the equilibrium value $\phi_{ij,0}$,

$$U_{\text{rep}} = \sum_i F\left[\sum_{j(i)} \phi_{ij}\right] \quad \text{with} \quad F[x] = \sum_{\alpha=1}^{4} A_\alpha x^\alpha. \tag{2}$$

The embedding coefficients A_α are those of Table 1 in Ref. 8. For large arguments this embedding function is dominated by the quartic term with a tiny, but negative, coefficient, which turns the repulsion into attraction. Therefore, we replace the embedding function by a linear function $F[x] = x/2$ for large arguments beyond the turning point $x = 105$.

When bonds are formed between *sp*-valent atoms, the electronic occupation of the *s* and *p* states may change. Assuming that the atoms remain charge neutral, the associated promotion energy can be expressed as the product of the energy difference $\delta_i = E_{ip} - E_{is}$ between the *s* and *p* states and the change ΔN_{ip} in the number of electrons populating the *p* states, as compared to the isolated atom,

$$U_{\text{prom}} = \sum_i \delta_i \Delta N_{ip}. \tag{3}$$

The attractive bond energy can be expressed as a sum over bonds in terms of the Hamiltonian and the bond-order matrix,

$$U_{\text{bond}} = \frac{1}{2} \sum_{i,j(i)} U_{\text{bond}}^{ij} = \sum_{i,j(i)} \text{Tr}(\hat{\Theta}_{ji} \hat{H}_{ij}), \tag{4}$$

where the prefactor 1/2 is compensated by the spin degeneracy. The intersite elements of the Hamiltonian matrix are those given by Slater and Koster[9] in terms of the fundamental two-center integrals and direction cosines. Using a minimal *sp* basis set and choosing the *z* axis of quantization along the bond axis from atom *i* to *j*, the intersite Hamiltonian matrix takes an especially simple form and can be split into a σ and a π block:

$$U_{\text{bond}}^{ij} = 2 \, \text{Tr}\left[\begin{pmatrix} \Theta_{js,is} & \Theta_{js,iz} \\ \Theta_{jz,is} & \Theta_{jz,iz} \end{pmatrix}\begin{pmatrix} ss\sigma_{ij} & sp\sigma_{ij} \\ ps\sigma_{ij} & pp\sigma_{ij} \end{pmatrix}\right]$$
$$+ 2 \, \text{Tr}\left[\begin{pmatrix} \Theta_{jx,ix} & \Theta_{jx,iy} \\ \Theta_{jy,ix} & \Theta_{jy,iy} \end{pmatrix}\begin{pmatrix} pp\pi_{ij} & 0 \\ 0 & pp\pi_{ij} \end{pmatrix}\right], \tag{5}$$

where $\{ss\sigma_{ij}, sp\sigma_{ij}, ps\sigma_{ij}, pp\sigma_{ij}, pp\pi_{ij}\}$ are the fundamental two-center integrals. Their distance dependence is described by the same scaling function $s(r_{ij})$ as used for the pairwise repulsion ϕ_{ij}, and is separated from the corresponding equilibrium values, e.g., $ss\sigma_{ij} = ss\sigma_{ij,0}s(r_{ij})$. To further simplify

the matrix product of the σ block, bonding and antibonding hybrid states can be introduced with an orthogonal transformation. The s and z states are combined in such a way that only the hopping integral $\beta_{\sigma,ij} = \langle i\sigma | \hat{H} | j\sigma \rangle$ between bonding hybrids on neighboring atoms does not vanish:

$$
\begin{aligned}
|i\sigma\rangle &= \sqrt{1 - p_{\sigma,i}}|is\rangle + \sqrt{p_{\sigma,i}}|iz\rangle, \\
|i\sigma_0\rangle &= \sqrt{p_{\sigma,i}}|is\rangle - \sqrt{1 - p_{\sigma,i}}|iz\rangle, \\
|j\sigma\rangle &= \sqrt{1 - p_{\sigma,j}}|js\rangle - \sqrt{p_{\sigma,j}}|jz\rangle, \\
|j\sigma_0\rangle &= \sqrt{p_{\sigma,j}}|js\rangle + \sqrt{1 - p_{\sigma,j}}|jz\rangle.
\end{aligned}
\tag{6}
$$

In the reduced TB model[10,11] the $sp\sigma$ integral is approximated by the geometric mean of the $ss\sigma$ and $pp\sigma$ integrals. Assuming that the $ss\sigma$ and $pp\sigma$ integrals show the same distance dependence, the four independent TB integrals $\{ss\sigma_{ij}, pp\sigma_{ij}, sp\sigma_{ij}, ps\sigma_{ji}\}$ can be given in terms of only three parameters $\{\beta_{\sigma,ij}, p_{\sigma,i}, p_{\sigma,j}\}$:

$$
|\beta_{\sigma,ij}| \begin{cases}
-\sqrt{(1 - p_{\sigma,i})(1 - p_{\sigma,j})} = ss\sigma_{ij}, \\
\sqrt{p_{\sigma,i} p_{\sigma,j}} = pp\sigma_{ij}, \\
\sqrt{(1 - p_{\sigma,i}) p_{\sigma,j}} = sp\sigma_{ij}, \\
-\sqrt{p_{\sigma,i}(1 - p_{\sigma,j})} = ps\sigma_{ij},
\end{cases}
\tag{7}
$$

where the species-dependent constant[12] p_σ describes the mixture of s and p states in the hybrids of Eq. (6),

$$
p_{\sigma,i} = \frac{pp\sigma_{ii}}{|ss\sigma_{ii}| + pp\sigma_{ii}}.
\tag{8}
$$

The bond energy is now determined by single σ- and π-bond orders, $\Theta_{\sigma,ji} \equiv \Theta_{j\sigma,i\sigma}$ and $\Theta_{\pi,ji} \equiv \Theta_{jx,ix} + \Theta_{jy,iy}$, and reads

$$
U_{\text{bond}}^{ij} = 2(\Theta_{\sigma,ji}\beta_{\sigma,ij} + \Theta_{\pi,ji}\beta_{\pi,ij}),
\tag{9}
$$

where $\beta_{\pi,ij} = pp\pi_{ij}$ denotes the π-bond integral. This expression still requires exact diagonalization of the Hamiltonian, since the bond orders are given in terms of the expansion coefficients of the eigenstates. However, for covalently bonded systems with a half-filled valence band the bond orders can be approximated with many-atom expansions as outlined in the next section. Before we proceed, we have to note that the reduced bond energy of Eq. (9) will differ from that given by exact diagonalization of the conventional TB Hamiltonian. To compensate this, we shift all two-center hopping integrals of the σ block in Eq. (5) by ξ. This fitting parameter affects only the hybrid bond integral β_σ as defined in Eq. (7), but cancels in the definition of the hybridization parameter p_σ. For notational convenience ξ will be absorbed into β_σ, all occurrences of which have to be understood accordingly:

$$
\xi\beta_\sigma \Rightarrow \beta_\sigma.
\tag{10}
$$

III. BOND ORDER

Pettifor *et al.* have derived[4,5,11] an analytical expression for the σ-bond order. They started from the representation of

the bond order as a complex integral[13] with E_f as the Fermi energy and $i\eta$ as an imaginary infinitesimal,

$$
\Theta_{i\sigma,j\sigma} = -\frac{1}{\pi} \lim_{\eta \to 0} \text{Im} \int^{E_f} dE \, G_{i\sigma,j\sigma}(E + i\eta),
\tag{11}
$$

and restricted the poles of the intersite Green function G_{ij} to be the same as those of the average on-site Green functions $(G_{ii} + G_{jj})/2$. Using a Lanczos transformation,[14] the on-site element $G_{ii}(E) = \langle i | (E - \hat{H})^{-1} | i \rangle$ of the Green function could then be evaluated recursively, resulting in a continued fraction.[15] The recursion was taken to four levels and the integral of Eq. (11), evaluated in the complex plane as a sum over the residues, related to the four poles of the Green function. For a half-filled band only the two lowest poles are occupied, and the bond order was expressed in terms of the recursion coefficients. Finally, these recursion coefficients were related to the moments $\mu_{n\sigma}^i$ of the projected density of states $D_{i\sigma}(E)$,

$$
\begin{aligned}
\mu_{n\sigma}^i &= \int (E - H_{i\sigma,i\sigma})^n D_{i\sigma}(E) dE \\
&= \sum_{\alpha_1,\dots,\alpha_{n-1}} H_{i\sigma,\alpha} H_{\alpha,\alpha_1} \cdots H_{\alpha_{n-1},i\sigma}.
\end{aligned}
\tag{12}
$$

This so-called moments theorem[16] allows one to evaluate the nth moment with respect to a given state (here the hybrid $|i\sigma\rangle$) as a sum of closed paths with hoppings to states $\alpha_1, \dots, \alpha_{n-1}$, where the compound index α includes atom and state indices. Paths extending out to states on neighboring atoms make it a many-atom expansion. It is this equation on which our extensions are based. Assuming a symmetric density of states with vanishing odd moments, the bond order could be written in a very compact form:

$$
\Theta_{i\sigma,j\sigma}^{\text{BOP4+}} = 1 / \sqrt{1 + \frac{\Phi_{2\sigma}^i + \Phi_{2\sigma}^j + \tilde{\Phi}_{2\sigma}^i \tilde{\Phi}_{2\sigma}^j (2 + \Delta\tilde{\Phi}_{4\sigma})}{(1 + \Delta\tilde{\Phi}_{4\sigma})^2}},
\tag{13}
$$

$$
\Delta\Phi_{4\sigma} = \frac{\Phi_{4\sigma}^i + \Phi_{4\sigma}^j - (\Phi_{2\sigma}^i)^2 - (\Phi_{2\sigma}^j)^2}{\Phi_{2\sigma}^i + \Phi_{2\sigma}^j},
$$

$$
\tilde{\Phi}_{2\sigma}^i \tilde{\Phi}_{2\sigma}^j = \Phi_{2\sigma}^i \Phi_{2\sigma}^j / \sqrt{\Delta\Phi_{4\sigma} + \Phi_{2\sigma}^i \Phi_{2\sigma}^j},
$$

$$
\Delta\tilde{\Phi}_{4\sigma} = \Delta\Phi_{4\sigma} / \sqrt{\Delta\Phi_{4\sigma} + \Phi_{2\sigma}^i \Phi_{2\sigma}^j}.
\tag{14}
$$

Here the hoppings $\beta_{\sigma,ij}$ back and forth between the σ hybrids on the bonding neighbors i and j have been separated from the remaining paths of Eq. (12), since they are normalized to unity by the σ-bond integral:

$$
\hat{\mu}_{4\sigma}^i = \mu_{4\sigma}^i / \beta_{\sigma,ij}^4 = \Phi_{4\sigma}^i + 1 + (2\Phi_{2\sigma}^i + \Phi_{2\sigma}^j),
\tag{15}
$$

$$
\hat{\mu}_{2\sigma}^i = \mu_{2\sigma}^i / \beta_{\sigma,ij}^2 = 1 + \Phi_{2\sigma}^i.
\tag{16}
$$

Note that the numerator in Eq. (13) does not contain the four-member ring term, introduced earlier[17] to model close-packed phases. The bond order would no longer be a real

TABLE I. Comparison of the contributions (20), (28), and (30) to the normalized fourth moment $\Phi_{4\sigma}$ for silicon and carbon in the cubic diamond phase. Carbon parameters are taken from Ref. 20.

	Carbon	Silicon
δ	6.7	6.45
β_σ	−10.016	−4.6266
p_σ	0.5238	0.6115
p_π	0.1548	0.2324
(20a)	0.012	0.213
(20b)	0.273	0.102
(20c)	0.165	0.038
(20d)	0.074	0.010
(28)	0.023	0.072
(30)	0.091	0.141
(31)	0.148	0.581

number if a negative ring term were dominating the numerator (which happens when the normalizing bond integral $\hat{\beta}_{\sigma,ij}$ is orders of magnitude smaller than the other bond integrals).

Evaluating a self-returning path of length 2, hoppings to states on neighboring atoms $k(i) \neq j$ have to be considered. This involves the direction cosines mentioned before which can be combined in an angular function. If the π-bond integrals are neglected, this function reads

$$g_{\sigma,jik} = 1 + (\cos\theta_{jik} - 1)p_{\sigma,i}. \quad (17)$$

In addition to hopping to neighbors, only the hopping to the antibonding hybrid and back needs to be considered, giving a term proportional to the energy splitting δ_i:

$$\hat{\delta}_i^2 = (H_{i\sigma,i\sigma_0})^2/\beta_{\sigma,ij}^2 = p_{\sigma,i}(1 - p_{\sigma,i})\delta_i^2/\beta_{\sigma,ij}^2. \quad (18)$$

On-site energies of the hybrids vanish, if the first moment $\mu_{1\sigma}^i = \langle i\sigma|\hat{H}|i\sigma\rangle \equiv 0$ is chosen as the energy zero,

TABLE II. Comparison of different BOP4 approximations to the σ-bond order with the respective TB values for silicon (see text). The reduced TB parameter β_σ is −5.0398 for the graphitic and −4.6266 for the diamond phase; other parameters as given in Table I.

Phase	δ	β_π	$\Theta_\sigma^{\text{BOP4}}$	$\Theta_\sigma^{\text{TB}}$
Diamond	6.45	−1.075	0.840	0.866
	6.45	0.00	0.832	0.902
	0.00	0.00	0.976	0.978
Graphite	6.45	−1.171	0.877	0.886
	6.45	0.00	0.851	0.882
	0.00	0.00	0.997	0.997

$$\Phi_{2\sigma}^i = \hat{\delta}_i^2 + \sum_{k(i)\neq j} g_{\sigma,jik}^2 \hat{\beta}_{\sigma,ik}^2. \quad (19)$$

As before, capped quantities are understood to be normalized by the σ-bond integral of the central bond, e.g., $\hat{\beta}_{\sigma,ik} = \beta_{\sigma,ik}/\beta_{\sigma,ij}$.

The self-returning path of length 4 can be split[5] into a contribution from on-site hoppings (20a), repetitive hoppings to the neighboring atoms $k(i) \neq j$ (20b), hoppings to two neighboring atoms $k(i) \neq j$ and $l(i) \neq j, k$ (20c), and hoppings extending out to a neighbor's neighbor $l(k) \neq i, j$ via the neighbor $k(i) \neq j$ (20d),

$$\Phi_{4\sigma}^i = \hat{\delta}_i^4 \quad (20a)$$

$$+ \sum_{k(i)\neq j} \hat{\beta}_{\sigma,ik}^4 g_{\sigma,jik}^2 \quad (20b)$$

$$+ \sum_{k(i)\neq j} \sum_{l(i)\neq j,k} \hat{\beta}_{\sigma,ik}^2 \hat{\beta}_{\sigma,il}^2 g_{\sigma,jik} g_{\sigma,kil} g_{\sigma,jil} \quad (20c)$$

$$+ \sum_{k(i)\neq j} \sum_{l(k)\neq i,j} \hat{\beta}_{\sigma,ik}^2 \hat{\beta}_{\sigma,kl}^2 g_{\sigma,jik}^2 g_{\sigma,ikl}^2. \quad (20d)$$

Note that, in order to conform with our derivation in the next section, the on-site hoppings $\hat{\delta}$ are integral parts of the paths $\Phi_{4\sigma}$ and $\Phi_{2\sigma}$, whereas Pettifor and Oleinik listed them separately in the expression for the bond order after neglecting all cross terms between $\hat{\delta}$ and $\hat{\beta}_\sigma$ [see Eq. (9) of Ref. 5].

For the π-bond order a similar expression was given:[4]

$$\Theta_{\pi,ji} = 1/\sqrt{1 + \Phi_{2\pi} - \Phi_{4\pi}^{1/2}} + 1/\sqrt{1 + \Phi_{2\pi} + \Phi_{4\pi}^{1/2}}. \quad (21)$$

To compare the strengths of π and σ bonds, the ratio

$$p_{\pi,ij} = \beta_{\pi,ij}/\beta_{\sigma,ij} \quad (22)$$

is defined in analogy to Eq. (8). Assuming[11]

$$p_\pi^2 \ll p_\sigma, \quad (23)$$

the self-returning paths of lengths 2 and 4 were given as

$$\Phi_{2\pi} = \frac{1}{2}\sum_{k(i)\neq j}(\sin^2\theta_{jik}\hat{\beta}_{ik}^2 + 2\hat{\beta}_{\pi,ik}^2) + \frac{(i \leftrightarrow j)}{2}, \quad (24)$$

$$\Phi_{4\pi} = \frac{1}{4}\left(\sum_{k(i),l(i)\neq j}\sin^2\theta_{jik}\sin^2\theta_{jil}\cos(2\varphi_{kl})\hat{\beta}_{ik}^2\hat{\beta}_{il}^2 \right.$$
$$\left. + \sum_{\substack{k(i)\neq j \\ l(j)\neq i}}\sin^2\theta_{jik}\sin^2\theta_{ijl}\cos(2\varphi_{kl})\hat{\beta}_{ik}^2\hat{\beta}_{jl}^2\right) + \frac{(i \leftrightarrow j)}{4},$$
$$(25)$$

with

$$\hat{\beta}_{ik}^2 = p_{\sigma,i}\hat{\beta}_{\sigma,ik}^2 - \hat{\beta}_{\pi,ik}^2. \quad (26)$$

In contrast to Eqs. (19) and (20), the capped bond integrals in Eqs. (24) and (25) are understood to be normalized by the π-bond integral $\beta_{\pi,ij}$. For the sake of compactness the term

$(i \leftrightarrow j)$ represents an additional sum similar to the preceding sum in parentheses, but with interchanged indices i and j. The angle of torsion φ_{kl} of the bonds to atoms k and l is taken in the projection on the plane perpendicular to reference bond ij and can conveniently be obtained from the direct angle $\theta_{k,l}$ between these bonds, using $\cos(2\varphi) = \cos^2\varphi - 1$ and the relation[18]

$$\cos \varphi_{kl} = \frac{\cos \theta_{k,l} - \cos \theta_{jik} \cos \theta_{jil}}{\sin \theta_{jik} \sin \theta_{jil}}. \qquad (27)$$

IV. EXTENDED BOND ORDER

The self-returning path of length 4 in Eq. (20) has been evaluated, assuming that intersite hoppings with π-bond character can generally be neglected. If terms proportional to the π-bond integral are retained using the assumption (23), a hopping to a neighbor's neighbor $l(k) \neq i,j$ via the neighbor $k(i) \neq j$ will give[19] an additional, significant contribution to the overall fourth moment, similar to that given in Eq. (20d):

$$\sum_{k(i) \neq j} \sum_{l(k) \neq i,j} \hat{\beta}^2_{\sigma,ik} \hat{\beta}^2_{\sigma,kl} (2g_{\sigma,jik}g_{\sigma,ikl} + g_{\varphi,jl})g_{\varphi,jl}. \qquad (28)$$

This term introduces a torsional stiffness to the σ-bond order via

$$g_{\varphi,jl} = p_{\pi,ik}\sqrt{p_{\sigma,i}p_{\sigma,k}}\cos \varphi_{jl} \sin \theta_{jik} \sin \theta_{ikl}, \qquad (29)$$

previously known only for the π-bond order.

As mentioned above, the on-site hybrid energies, which depend on the absolute energies of the s and p states, vanish by setting the energy zero to $\mu^i_{1\sigma} \equiv 0$. Similarly, hybrid energies on other atoms also vanish. The bond order then depends only on the relative energy difference δ due to coupling between bonding and antibonding hybrids of the same atom. We further generalize the evaluation of the self-returning paths of length 4 by including cross terms between on-site and intersite hoppings and extend Eq. (20) with

$$\sum_{k(i) \neq j} \hat{\beta}^2_{\sigma,ik} g^2_{\sigma,jik}(2\hat{\delta}^2_i + \hat{\delta}^2_k), \qquad (30)$$

where we have neglected π-bond integrals as done previously in Eq. (17). The first term of Eq. (30) is proportional to $\hat{\delta}^2_i$ and corresponds to an intersite hopping to a neighboring atom k and back followed by an on-site hopping to the antibonding hybrid and back, where the factor 2 results from the inverse scenario. The on-site hopping may of course also take place at the neighboring site k, giving the second contribution proportional to $\hat{\delta}^2_k$. An on-site hopping to the antibonding state followed by an intersite hopping to a neighboring atom and back will give another term proportional to $\hat{\delta}^2_i$,

$$\sum_{k(i) \neq j} \hat{\beta}^2_{\sigma,ik} p_{\sigma,i}(1 - p_{\sigma,i})(1 - \cos \theta_{jik})^2 \hat{\delta}^2_i. \qquad (31)$$

Note, that the neighbor $k(i) = j$ is excluded, since Eq. (31) vanishes for this case and the two terms in Eq. (30) have already been accounted for by the self-returning paths of length 2, when the fourth moment is constructed in Eq. (15).

The magnitudes of the individual contributions are compared in Table I. The fourth moment is dominated by the on-site contributions of Eqs. (20a), (30), and (31), if the energy splitting δ is larger than the absolute value of the energy β_σ, associated with the hopping between σ hybrids on neighboring atoms, as is the case for silicon. While the π-enhanced contribution (28) is rather marginal (4.5%) due to the relatively strong σ bonds in carbon, it is comparable to the pure σ contributions (20b)–(20d) for silicon (48%).

This can also been seen in Fig. 1, where σ and π contributions to hopping to the next nearest neighbor are compared for silicon with equal bond lengths and bonds ij and ik fixed at the tetrahedral angle $\cos \theta_{jik} = -1/3$, typical for diamond systems, while the bond angle θ_{ikl} remains free. After fixing also the latter angle at $\cos \theta_{ikl} = -1/3$, the bond kl may still move on a cone around the bond ik. This last degree of freedom can be described by the angle of torsion φ, which is not captured by the pure σ contribution (see Fig. 2).

To assess the influence of the on-site and π terms, we compare the analytical bond orders of different approximations with TB values in Table II. The TB value for each model was obtained by exact diagonalization using the OXON program, setting the energy splitting and π-bond integral to the indicated values. The TB bond order is rather well approximated by the BOP4 with the simplifying assumptions $\delta = 0$ and $\beta_\pi = 0$ [see Eq. (68) in Ref. 21]. However, if the energy splitting is taken into account, the BOP4 expression, neglecting cross terms of $\hat{\delta}$ and $\hat{\beta}_\sigma$, underestimates the bond order [see Eq. (9) of Ref. 5]. The σ-bond order of a realistic TB model with nonvanishing π bonds and energy splitting is best described by the present approximation, BOP4$^+$.

V. PARAMETRIZATION

Before the parametrization can be described, the expression for the promotion energy needs to be specified. Since the expansion coefficients and the occupations of the eigenstates are not known, the change in the occupation of the atomic p state of Eq. (3) was approximated with an asymptotic function of the average strength of the hybrid bonds β_σ [Ref. 11 and Eq. (108) of Ref. 4].

Since this leads to unphysical promotion energies for cluster atoms such as the atoms at the center of an isolated diamond pyramid, we have empirically modified the func-

TABLE III. Potential parameters of Eqs. (7), (8), (32), and (33) for silicon interactions as given in Ref. 23; energy splitting δ and Slater-Koster integrals are given in eV, distances r in Å.

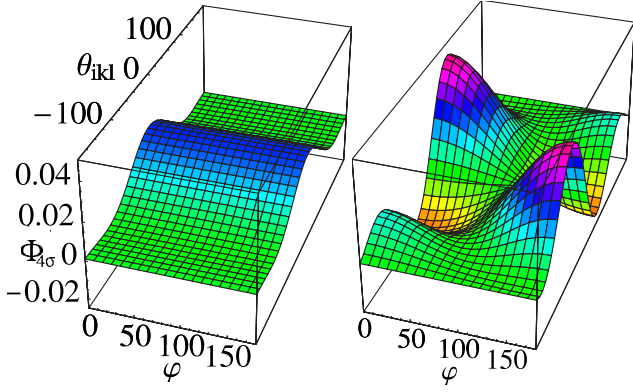| δ	$ss\sigma_0$	$pp\sigma_0$	$pp\pi_0$	r_{on}	r_{off}	r^{rep}_{cut}	r^{SK}_{cut}
6.45	−1.938	3.050	−1.075	3.300	3.700	3.8521	3.8661

FIG. 1. (Color online) Contributions to the path of length 4 for silicon, starting and ending on atom i and extending to a neighbor's neighbor $l(k(i)) \neq i,j$ with atoms j, i, and k forming a tetrahedral bond angle $\cos \theta_{jik} = -1/3$; unlike the pure σ term [Eq. (20d), left panel] the π term [Eq. (28), right panel] depends on the angle of torsion φ (parameters from Table I).
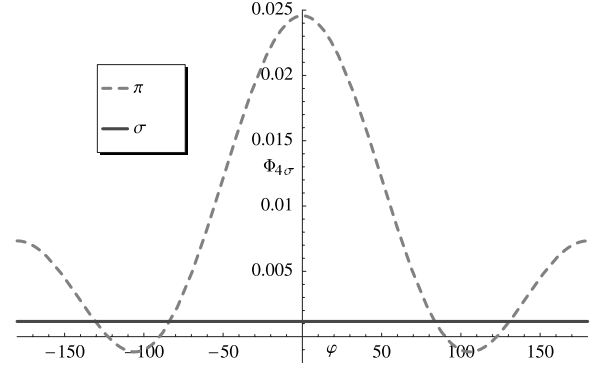

FIG. 2. Superposition of the contributions depicted in Fig. 1, sliced at the bond angle $\cos \theta_{ikl} = -1/3$. All bond angles are fixed, as the bond kl moves on a cone around the bond ik. The pure σ term [Eq. (20d), solid line] remains constant, while the π term [Eq. (28), dashed line] depends on the angle of torsion φ and has a maximum at the planar configuration with $\varphi = 0°$, as found in hexagonal diamond.

tional form. We want to motivate this by recalling the origin of electronic promotion as follows. To promote an sp-valent atom from an s^2p^2 to an sp^3 configuration, energy needs to be invested that is proportional to the splitting δ. This investment may well be exceeded by the energy gain due to the newly formed bonds in the promoted configuration. The ratio of the invested and gained energy determines the probability of an atom to be found in the promoted configuration, which may also be interpreted as the fractional promotion of the electron. Based on a least-squares fit to the promotion energy obtained from exact TB calculations, we have investigated various functional forms to combine the initial atomic and final bond energies and chose Eq. (32), which approximates the energy gain for an atom by the sum of the hybrid bonds β_σ rather than their average,

$$\Delta N_{ip} = 1 - 1/\sqrt{1 + y_i} \quad \text{with } y_i = \frac{\kappa_i}{4\delta_i^2} \sum_{k(i)} \frac{\beta_{\sigma,ik}^2}{\xi_{ik}^2}. \quad (32)$$

To decouple the promotion parameter κ from the reduction parameter ξ, the shifted bond integral of Eq. (10) is divided by ξ. Equation (32) represents only a small modification of Eq. (108) of Ref. 4 and the two approximations give the same promotion energy for atoms with four neighbors. To recall this fact, the prefactor 1/4 has been separated from the fit parameter κ.

The two approximations for the promotion energy are compared[20] for some hydrocarbon molecules and carbon systems in Fig. 3. While Eq. (32) underestimates the large promotion energies for systems with strong π bonds such as

C_2H_2, C_2H_4, and graphite, it represents an improvement for undercoordinated systems such as the isolated dimer. This is especially remarkable for the central atom $\text{dia}_{5,4,3}^z$ of an isolated diamond pyramid, where Eq. (108) of Ref. 4 incorrectly predicts identical values.

Following Godwin, Skinner, and Pettifor,[22] the distance dependences of the pairwise repulsion in Eq. (2) as well as the fundamental Slater-Koster integrals in Eq. (5) are modeled with the same scaling function,

$$s(r) = \left(\frac{r_0}{r}\right)^{n^x} \exp\left\{n^x\left[\left(\frac{r_0}{r_{\text{cut}}^x}\right)^{n_c^x} - \left(\frac{r}{r_{\text{cut}}^x}\right)^{n_c^x}\right]\right\}, \quad (33)$$

which is centered at r_0, i.e., $s(r_0) = 1$. The fit parameters n^x and n_c^x as well as the cutoff distance r_{cut} are different for the repulsive scaling ($x=\text{rep}$) and the Slater-Koster scaling ($x=\text{SK}$), denoted by the respective superscripts in Tables III and IV. To smoothly cut off the interaction between first and second neighbor distance, a cubic spline replaces the scaling function in the interval $[r_{\text{on}}, r_{\text{off}}]$ with $\Delta = r - r_{\text{on}}$, such that

$$s_c(r) = s_0 + s_1\Delta + s_2\Delta^2 + s_3\Delta^3,$$

$$s(r) = \begin{cases} s(r) & (r < r_{\text{on}}), \\ 0 & (r_{\text{off}} < r), \\ s_c(r) & (\text{else}). \end{cases} \quad (34)$$

The coefficients $s_0, \ldots, s_3$ are fixed by requiring a match of the functions and their first derivatives at the control points r_{on} and r_{off}:

TABLE IV. Fit parameter of Eqs. (2), (32), and (33) for silicon interactions, optimized to fit equilibrium values and curvatures of the cohesive energy of cubic diamond at $a_0 = 5.429$ Å and the secondary β-Sn phase. The scaling functions are centered at the equilibrium bond length of diamond, i.e., $r_0 = 2.3508$ Å.

ϕ_0	ξ	κ	n^{SK}	n_c^{SK}	n^{rep}	n_c^{rep}
4.09119	0.927548	5.79	1.642565	7.067494	3.895511	7.254549

TABLE V. Properties obtained with BOP4$^+$ in comparison with results from exact diagonalization (TB) and experiments for silicon in the cubic diamond phase: explicitly fitted values are indicated by (*). The elastic constant C_{44}^0 is obtained for fixed (unrelaxed) inner coordinates after the shear is applied.

Model	B (Mbar)	C_{44}^0 (C_{44}) (Mbar)	C' (Mbar)	a_0 (Å)	$E_{coh}^{\diamond}$ (eV)
TB	0.998	1.099	0.362	5.429	5.99
BOP4$^+$	0.987*	1.074 (0.888)	0.294	5.429*	4.63*
Expt.	0.99	1.110 (0.796)^a	0.509^a	5.429^b	4.63^c

[a]References 24 and 25.
[b]Reference 26 at 0 K.
[c]References 27 and 28.

$$s_c(r_{on}) = s(r_{on}), \qquad s_c(r_{off}) = 0,$$
$$s'_c(r_{on}) = s'(r_{on}), \qquad s'_c(r_{off}) = 0. \qquad (35)$$

The interatomic BOP4$^+$ potential is given by Eqs. (1)–(4) and (9) together with the analytical expressions for the bond orders and the promotion energy in Eqs. (13), (21), and (32). The TB parameters for silicon interactions are based on the orthogonal parametrization of Bowler *et al.* (see Table III and Ref. 23).

We now briefly describe the fitting procedure. First, the reduced bond energy is fitted by shifting the σ-bond integral as in Eq. (10). Next we adjust the parameter κ to fit the promotion energy of Eqs. (32) and (3) to that from exact TB calculations. The reduction parameter ξ as well as the promotion parameter κ are determined for a cubic diamond system with bond lengths at the experimental reference value. We choose to center the scaling function (33) at this equilibrium bond length to decouple the equilibrium parameters κ, ξ, and ϕ_0 from the four scaling parameters $n^{rep}, n_c^{rep}, n^{SK}, n_c^{SK}$. However, to be able to fit the equilibrium value and the curvature of the cohesive energy of the primary phase as well as the relative atomic volume and energy difference of the secondary phase, the repulsive equilibrium parameter ϕ_0 of Eq. (2) and the four scaling parameters were tuned simultaneously using a Metropolis conjugate-gradient algorithm. The seven fit parameters are given in Table IV. The fitted
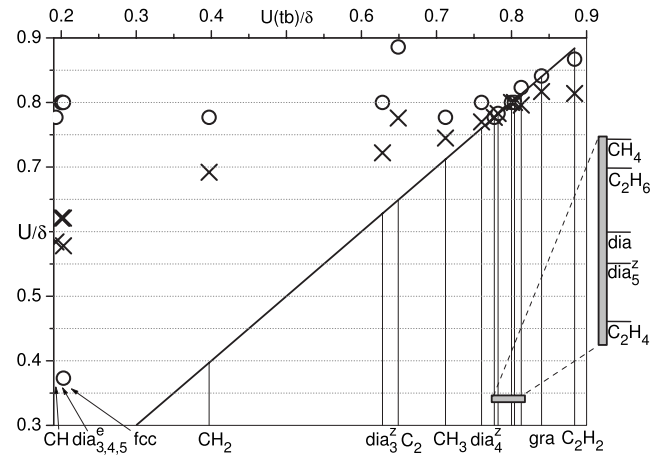

FIG. 3. Promotion energy for carbon and hydrocarbon systems as given by Eq. (32) (crosses) and Eq. (108) of Ref. 4 (circles) compared with exact tight-binding results. dia$_{3,4,5}^e$ and dia$_{3,4,5}^z$ represent the carbon atoms at the edge or the center of the cluster of three, four, or five atoms, which result from the isolated five-atom pyramid with diamondlike bond lengths and four, angles after removing none, one, or two edge atoms, respectively.

cohesive energy and bulk modulus of cubic diamond and β-Sn as a secondary phase are compared in Tables V and VI. For our TB calculations we have used the parametrization of Bowler *et al.*[23]

To test the transferability of the potential, the Si(001) surface and the neutral monovacany have been studied. Due to the extensions the BOP4$^+$ correctly describes the $p(2 \times 2)$ reconstruction with asymmetrically buckled surface dimers as the energetically most stable reconstruction. Energies and dimer lengths are compared in Table VII with other empirical potentials as well as TB and LDA results. The reduced TB calculations (which use the same parametrization as the BOP4$^+$) demonstrate how the approximate expressions for the bond order and the promotion energy affect the surface reconstructions. Our simulations were carried out using a 4 $\times 4 \times 1$ supercell containing 128 atoms, while assuming periodic boundaries in the extended directions x and y only. Additionally, the 32 atoms of the lowest of the four layers

TABLE VI. Relative atomic volumes $\bar{V}_{min} = V_{min}/V_{min}^{\diamond}$ and energy differences $\Delta E = E_{min} - E_{min}^{\diamond}$ (given in eV) for some silicon structures calculated with BOP4$^+$ and compared to local density approximation (LDA) (Refs. 28–30) and exact tight binding results: explicitly fitted values are indicated by (*). Note that the BOP4$^+$ is unable to distinguish the hexagonal (alias Lonsdaleite) from the cubic diamond phase (Ref. 19). The axis ratio of the lattice constants is $c/a = 0.5516$ for the β-Sn phase and $c/a = 2.726$ for the hypothetical graphite phase as found for graphitic carbon.

	Phase									
	Lonsdaleite		Graphite		β-Sn		sc		fcc	
Model	ΔE	$\bar{V}_{min}$	ΔE	$\bar{V}_{min}$	ΔE	$\bar{V}_{min}$	ΔE	$\bar{V}_{min}$	ΔE	$\bar{V}_{min}$
LDA	0.016	1.003	0.71	1.75	0.27	0.76	0.35	0.79	0.57	0.72
TB	0.016	0.997	1.14	1.89	0.42	0.77	0.65	0.90	0.69	0.87
BOP4$^+$	0.000	1.000	0.68	1.91	0.25*	0.84*	0.21	0.88	0.40	0.85

TABLE VII. Relative energy gain per surface dimer and dimer length of some well known reconstructions of the silicon (001) surface: $\Delta E_{p(2\times1)}$ is given with respect to the ideal (1×1) surface and $\Delta E_{p(2\times2)}$ with respect to the $p(2\times1)$ reconstruction; values for the Stillinger-Weber (SW) and the Tersoff (T3) potential are taken from Ref. 31 and LDA results from Refs. 32 and 33. In the reduced TB model the $sp\sigma$ integral was replaced by the geometrical mean of the $ss\sigma$ and $pp\sigma$ integrals as noted in Sec. II.

Model	$\Delta E_{p(2\times1)}$ (eV/dimer)	$\Delta E_{p(2\times2)}$ (eV/dimer)	$r_{p(2\times1)}$ (Å)	$r_{p(2\times2)}$ (Å)
LDA	−1.86	−0.170	2.230	
TB	−0.85	−0.236	2.430	2.438
Reduced TB	−1.95	−0.457	2.645	2.661
BOP4$^+$	−2.30	−0.014	2.440	2.416
T3	−1.52		2.365	
SW	−1.80		2.404	

have been fixed to simulate a continuation into the bulk. To study the neutral monovacancy, we have used a periodic unit cell with 64 atoms. Due to its shallow energy hypersurface the neighboring atoms around the vacancy relax either in or outward, depending on their initial positions. The change $\Delta V = V^{\rm rel}/V^0 - 1$ of the volume of the tetrahedron, defined by the four atoms closest to the vacancy, as well as the (un)relaxed formation energies $E_{\rm vac} = E_{N-1} - (N-1)E_N/N$, are compared in Table VIII. Here E_{N-1} describes the energy of the system with the vacancy and E_N the reference energy of the perfect crystal.

VI. CONCLUSIONS

We have improved the analytic bond-order potential to include intermediate π bonds and on-site hoppings in the fourth-moment approximation to the σ-bond order and pro-

TABLE VIII. Comparison of formation energy and relative volume change for the neutral monovacancy in silicon with LDA and TB results as well as with empirical potentials from Tersoff (T3) and Stillinger and Weber (SW). While all models consistently predict a positive formation energy, only the Tersoff potential describes an outward relaxation of the atoms surrounding the vacancy.

Model	$E_{\rm vac}^0$ (eV)	$E_{\rm vac}^{\rm rel}$ (eV)	ΔV (%)
LDA (Ref. 34)		3.3	−41.4
TB	5.76	3.8	−46.9
BOP4$^+$	7.03	3.2	−28.3
T3 (Refs. 31 and 35)	4.10	3.7	+34.9
SW (Ref. 31)	4.63	2.8	−56.1
Expt. (Ref. 36)		3.6	

posed a modified expression for the promotion energy to better handle unsaturated bonds and enhance transferability. The potential was parametrized for silicon and its predictions are in good agreement with experimental and theoretical data. While the inclusion of the π and on-site extensions results in consistently better bond orders, the fit of the potential is somewhat compromised by the approximation of the promotion energy, for which an accurate and transferable expression is still needed.

The extensions make up less than 15% during the evaluation of the forces, which can be done in 134 μs for each of the 216 000 atoms of a cubic diamond structure with four nearest neighbors, using a Pentium IV processor clocked at 2 GHz. In comparison, this is an order of magnitude slower than the 14 μs, needed for force evaluation with the Tersoff potential. The BOP4$^+$ can be used to simulate systems with up to 10^6 atoms on a standard desktop computer equipped with 1 Gbyte of RAM. Applications of the potential in MD simulations of processes at the interface of bonded wafers with extended defects will be published elsewhere.[37]

*schee@mpi-halle.de

[1] K. Scheerschmidt, *Theory of Defects in Semiconductors* (Springer-Verlag, Berlin, 2006), Chap. 9, p. 195.

[2] M. Finnis, *Interatomic Forces in Condensed Matter* (Oxford Materials, New York, 2003), Chap. 7.

[3] D. Bowler, M. Aoki, C. Goringe, A. P. Horsfield, and D. Pettifor, Modell. Simul. Mater. Sci. Eng. **5**, 199 (1997).

[4] D. G. Pettifor and I. I. Oleinik, Phys. Rev. B **59**, 8487 (1999).

[5] D. G. Pettifor and I. I. Oleinik, Phys. Rev. Lett. **84**, 4124 (2000).

[6] A. Sutton, M. Finnis, D. Pettifor, and Y. Ohta, J. Phys. C **21**, 35 (1988).

[7] C. Xu, C. Wang, C. Chan, and K. Ho, J. Phys.: Condens. Matter **4**, 6047 (1992).

[8] A. P. Horsfield, P. D. Godwin, D. G. Pettifor, and A. P. Sutton, Phys. Rev. B **54**, 15773 (1996).

[9] J. Slater and G. Koster, Phys. Rev. **94**, 1498 (1954).

[10] D. Pettifor, in *Many-Atom Interactions in Solids. Proceedings of the International Workshop* (Springer-Verlag, Berlin, 1990), Vol. 48, p. 64.

[11] D. Pettifor, M. Finnis, D. Nguyen-Manh, D. Murdick, X. Zhou, and H. Wadley, Mater. Sci. Eng., A **365**, 2 (2004).

[12] R. Drautz, D. A. Murdick, D. Nguyen-Manh, X. Zhou, H. N. G. Wadley, and D. G. Pettifor, Phys. Rev. B **72**, 144105 (2005).

[13] A. P. Horsfield, A. M. Bratovsky, M. Fearn, D. G. Pettifor, and M. Aoki, Phys. Rev. B **53**, 12694 (1996).

[14] C. Lanczos, J. Res. Natl. Bur. Stand. **45**, 225 (1950).

[15] G. Grosso and G. Parravicini, *Solid State Physics* (Academic Press, San Diego, CA, 2000).

[16] F. Cyrot-Lackman, Adv. Phys. **16**, 393 (1967).

[17] D. G. Pettifor and I. I. Oleinik, Phys. Rev. B **65**, 172103 (2002).

[18] M. Allen and D. Tildesley, *Computer Simulation of Liquids* (Oxford University Press, Oxford, 1997).

[19] V. Kuhlmann, Ph.D. thesis, Martin-Luther-Universität Halle-Wittenberg, Halle, 2006, http://www.bibliothek.uni-halle.de

[20] I. I. Oleinik and D. G. Pettifor, Phys. Rev. B **59**, 8500 (1999).

[21] D. Pettifor and I. Oleynik, Prog. Mater. Sci. **49**, 285 (2004).

[22] L. Godwin, A. Skinner, and D. Pettifor, Europhys. Lett. **9**, 701 (1989).

[23] D. Bowler, M. Fearn, C. M. Goringe, A. P. Horsfield, and D. Pettifor, J. Phys.: Condens. Matter **10**, 3719 (1998).

[24] H. McSkimin and J. Andreatch, J. Appl. Phys. **35**, 2161 (1964).

[25] M. T. Yin and M. L. Cohen, Phys. Rev. B **26**, 3259 (1982).

[26] J. Donohue, *The Structure of Elements* (Wiley, New York, 1974).

[27] L. Brewer, Lawrence Berkeley Laboratory Technical Report No. LB-3720, 1977 (unpublished).

[28] M. T. Yin and M. L. Cohen, Phys. Rev. B **26**, 5668 (1982).

[29] M. T. Yin and M. L. Cohen, Phys. Rev. B **29**, 6996 (1984).

[30] S. Wang and H. Ye, J. Phys.: Condens. Matter **15**, L197 (2003).

[31] H. Balamane, T. Halicioglu, and W. A. Tiller, Phys. Rev. B **46**, 2250 (1992).

[32] A. Ramstad, G. Brocks, and P. J. Kelly, Phys. Rev. B **51**, 14504 (1995).

[33] I. P. Batra, Phys. Rev. B **41**, 5048 (1990).

[34] M. J. Puska, S. Pöyukkö, M. Pesola, and R. M. Nieminen, Phys. Rev. B **58**, 1318 (1998).

[35] J. Tersoff, Phys. Rev. Lett. **64**, 1757 (1990).

[36] G. Watkin and J. Corbett, Phys. Rev. **134**, A1359 (1964).

[37] T. Wilhelm, V. Kuhlmann, and K. Scheerschmidt, Phys. Status Solidi C **4**, 3115 (2007).